Astron. Astrophys. 316, 538–546 (1996)

ASTRONOMY
AND
ASTROPHYSICS

Spatial variation of >40 MeV/n nuclei fluxes observed during the Ulysses rapid latitude scan

B. Heber[1], **W. Dröge**[1], **P. Ferrando**[2], **L.J. Haasbroek**[3], **H. Kunow**[1], **R. Müller-Mellin**[1], **C. Paizis**[4], **M.S. Potgieter**[3], **A. Raviart**[2], **and G. Wibberenz**[1]

[1] Institut für Kernphysik, Universität Kiel, D-24118 Kiel, Germany
[2] CEA, DSM/DAPNIA/Service d'Astrophysique, C.E.Saclay, F-91191 Gif-sur-Yvette, France
[3] Space Research Unit, Potchefstroom University, 2520 Potchefstroom, South Africa
[4] Istituto di Fisica Cosmica CNR, Universitá di Milano, I-20133 Milano, Italy

Received 20 February 1996 / Accepted 6 June 1996

Abstract. In this paper we present fluxes of galactic cosmic ray nuclei with energies above 40 MeV/n observed by the Kiel Electron Telescope on board the Ulysses spacecraft during the fast scan from the South Pole (September 1994) to the North Pole (July 1995). This part of the Ulysses orbit gives us the unique opportunity to investigate spatial modulation of cosmic rays under solar minimum conditions. We show that during this time period temporal variations are well ordered with particle rigidity using 1 AU data from the University of Chicago particle instrument on board IMP8. The latitudinal variation is particularly strong for 38–125 MeV/n helium nuclei and decreases with increasing energy. In contrast, the spatial variation for protons is most dominant in the energy range of a few hundred MeV. Spatial effects are very small for some ten to one hundred MeV protons. The proton results are compared with predictions of a steady-state modulation model which takes into account modifications of the large scale heliospheric magnetic field and an increased level of cosmic ray scattering over the poles. We find that the model is in excellent agreement with the latitudinal variations of >2 GeV protons, whereas it does not reproduce the behaviour at low rigidities. We conclude that either the assumed rigidity dependence for the diffusion coefficients at low energies has to be modified or that time-dependent modulation effects dominate at low energies.

Key words: cosmic rays – Sun: particle emission – interplanetary medium

1. Introduction

A full understanding of solar modulation of galactic cosmic rays and the anomalous component requires knowledge of the 3-dimensional structure of the heliosphere. The Pioneer and Voyager spacecraft have probed the heliosphere to beyond 60 AU, but no spacecraft prior to Ulysses has provided direct observations from latitudes higher than ∼34° from the ecliptic plane. The basic physical processes that lead to the long-term modulation of cosmic rays in the heliosphere have been known for many years. Models have been developed incorporating effects of diffusion, gradient and curvature drifts in the heliospheric magnetic field, and convection and adiabatic deceleration in the solar wind (for an overview see Burger & Hattingh 1995, Potgieter 1995 and references therein). These are all subject to spatial and temporal variations in the dynamic heliosphere. However, our knowledge of the relative importance of the various processes is still incomplete. Observations of cosmic rays at high latitudes can be used to improve our understanding of modulation processes.

The Ulysses spacecraft was launched on October 6, 1990 in the declining phase of solar cycle 22. In February 1992 the spacecraft encountered the planet Jupiter, and began its journey out of the ecliptic plane using a Jupiter gravity assist. The manoeuvre placed the spacecraft into an orbit inclined by 80° with respect to the Sun's equator with an eccentricity of 0.6, enabling it to reach the previously unexplored high-latitude regions of the heliosphere. In the eleven months from September 1994, when the spacecraft was at a distance of ∼2.2 AU from the Sun, until August 1995, when the spacecraft was at a distance of 2.0 AU, Ulysses moved from 80°S to 80°N and crossed the ecliptic plane in March 1995 at a radial distance of 1.34 AU. Prior to the Ulysses mission it was widely believed that in the present phase of this solar cycle positively charged cosmic rays would be able to arrive more easily over the poles of the Sun than at lower latitudes (see McKibben 1989). In the present paper we investigate this question using data from the Ulysses COsmic and Solar Particle INvestigation Kiel Electron Telescope (COSPIN/KET). In a companion paper (Ferrando et al. 1996) the modulation of galactic electrons is investigated and com-

Send offprint requests to: B. Heber

Table 1. KET energy channels

particle	E_{min} MeV/n	E_{max} MeV/n	P_{mean} MV
proton	38	125	420
proton	125	250	800
proton	250	2000	2200
proton	>2000		8000
helium	38	125	800
helium	250	2000	2800
helium	>2000		15000

pared with results derived from a time dependent modulation model.

The KET measures protons and helium nuclei in the energy range from 6 MeV/n to above 2 GeV/n and electrons in the energy range from 3 MeV to some GeV (for a complete description of the KET instrument see Simpson et al. 1992). We present proton and helium nuclei measurements from the KET instrument in different energy channels as listed in Table 1, electron measurements are analysed in Ferrando et al. (1996). The mean rigidity $P_{\rm mean}$ has been calculated using a method described in Rastoin et al. (1996) for the modulation parameter Φ = 500 MV. In order to separate spatial from temporal variations in the galactic cosmic ray flux, we compare our results with data from the University of Chicago instrument (UoC) on board IMP-8 (38–75 MeV and >106 MeV protons, and 25–95 MeV/n helium nuclei) and from the UoC Climax neutron monitor.

2. Observations

The top panel of Fig. 1 shows the daily averaged counting rates of protons in the energy range of 38–125 MeV registered by KET from June 1994 to the beginning of 1996. The shaded areas indicate time periods when Ulysses was below 70°S (South Polar Pass) from June to November 1994 and above 70°N (North Polar Pass) from June to September 1995. In March 1995 Ulysses crossed the ecliptic plane. During this time period solar activity was low and the 38–125 MeV proton channel indicates that the galactic cosmic ray flux was not contaminated by solar or locally accelerated energetic particles. Even the particle flux of 5–25 MeV protons (not shown here) increased only once by more than a factor of 3. The second panel of Fig. 1 shows the counting rates of >106 MeV protons. The shape of the measured time profile shows the spatial modulation of protons as a function of Ulysses' latitude as discussed in detail in the following section and the periodic decreases of >106 MeV protons with a time period of ∼26 days. It is known that these decreases occur almost at all latitudes and reflect the influence of Corotating Interaction Regions (CIR), see for example Dröge et al. (1995), McKibben et al. (1995) and Sanderson (1995). However, as evidenced in the top panel, both effects vanish or are very small compared to the temporal recovery in the proton flux at some tens of MeV. The differences of the spatial variation as a function of energy and particle species will be discussed in more detail below. The third panel shows the 27-day averaged tilt angle separately for the northern and southern hemispheres, indicating the evolution of solar activity (Hoeksema, private communication, 1995). From this evolution it is reasonable to assume that the heliosphere was almost stationary during the time period of the Ulysses fast latitude scan.

3. Data analysis

One of the primary goals of the Ulysses mission was to measure the latitudinal distribution of galactic cosmic rays. For our analysis we used the KET counting rates of >38 MeV/n protons and helium nuclei in different energy windows. We assume that in the present phase of the solar cycle and in the inner solar system the variation of the cosmic ray flux is separable in time and space. This means that the time dependence is the same everywhere and convection corrections can be neglected. To distinguish between temporal and two-dimensional spatial variations we ought to compare the fluxes measured with identical instruments on three spacecraft separated in radial distance *and* heliographic latitude. Analyzing data from only two spacecraft separated in radial distance and heliographic latitude we calculate the temporal and spatial variations under the assumption that the radial and latitudinal *gradients* do not vary significantly in time and space. The UoC instrument on board IMP8 and the UoC Climax neutron monitor are used to determine the temporal recovery of galactic cosmic ray fluxes at 1 AU as discussed in Sect. 3.1. In Sect. 3.2 we calculate under the assumption made above the latitudinal enhancement of galactic cosmic rays over the poles of the Sun. In Sect. 4 we describe the model and discuss its results in comparison with the data. For comparison we also show results from a "standard" steady-state drift modulation model (Burger & Potgieter 1989), which calculates the latitudinal variation along the Ulysses trajectory using an Archimedian spiral heliospheric magnetic field (HMF).

3.1. Temporal variation

The increase of solar activity associated with the onset of solar cycle 23 is not expected to commence before 1996 or 1997, and in 1995 the fluxes of galactic cosmic rays are still increasing. Fig. 2 left panel shows the measured 1 AU counting rates in two different energy channels from September 1994 to August 1995. The upper and lower panels show the daily averaged counting rates C of the UoC Climac neutron monitor and 70–98 MeV protons, respectively. From the counting rate time profiles it is reasonable to assume that during the time period of Ulysses' fast latitude scan the temporal rate of increase, $\gamma(P_{\rm mean}) = 1/C \cdot \partial C/\partial t$ (in %/year) as a function of rigidity $P_{\rm mean}$ can be calculated by fitting

$$C(P_{\rm mean}, t) = C_0 \cdot \exp\left(\gamma\left(P_{\rm mean}\right) \cdot t\right) \quad (1)$$

to the data. The temporal rate of increase $\gamma(P_{\rm mean})$ in %/year as calculated by Eq. 1 for the different energy channels of the UoC instrument and the UoC Climax neutron monitor are summarized in Table 2 and shown in Fig. 2 right panel. As expected the temporal variation of nuclei decreases with increasing rigidity.

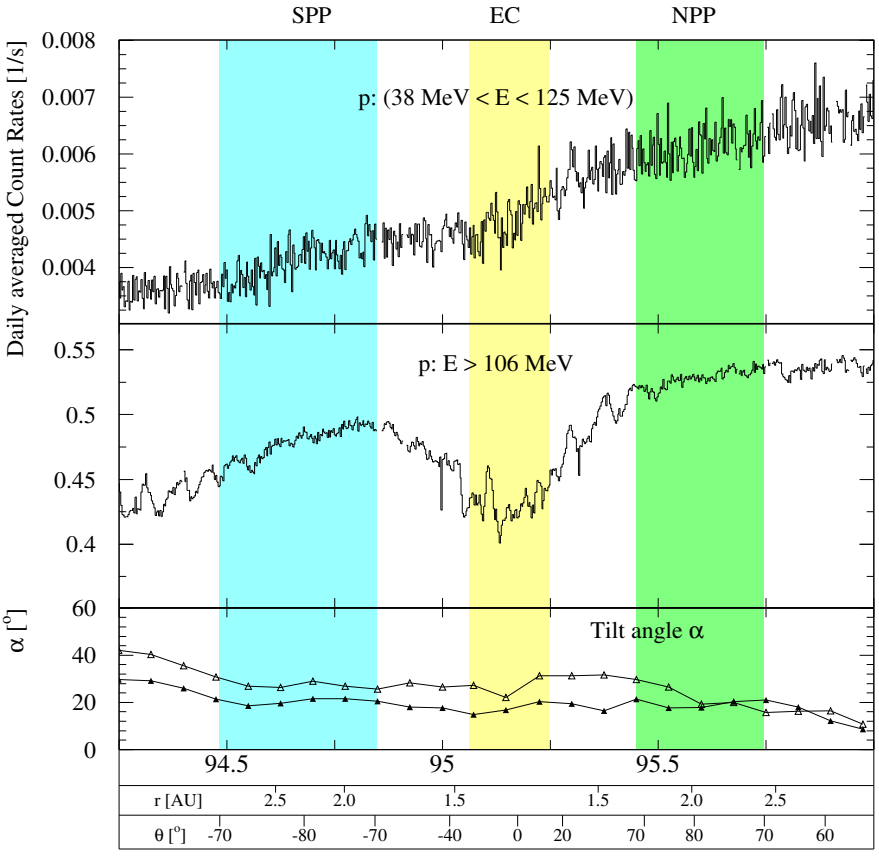

Fig. 1. Daily averaged counting rates from the KET instrument and 27-day averaged tilt angle for the northern (filled △) and southern (△) hemisphere. S.P.P. = southern polar passage, N.P.P. = northern polar passage.

Table 2. Upper and lower energy limits, weighted mean rigidity (P_{mean}, see Rastoin et al. 1996) and temporal rate of increase ($\gamma(P_{\mathrm{mean}})$) for protons, helium nuclei of the UoC instrument and the UoC Climax neutron monitor.

	E_{min} MeV/n	E_{max} MeV/n	P_{mean} MV	$\gamma(P_{\mathrm{mean}})$ %/year
proton	70	98	420	29.
proton	>106		2000	6.1
helium	25	90	600	14
Climax	>2200		10000–15000	0.8

The same result was reported by Heber et al. (1993) for the fast recovery of galactic cosmic ray fluxes in 1991 and 1992.

In order to determine the temporal variation in every KET channel we assume that the temporal rate of increase $\gamma(P_{\mathrm{mean}})$ can be approximated by:

$$\gamma(P_{\mathrm{mean}}) = \gamma_0 \cdot P_{\mathrm{mean}}^{\beta} \tag{2}$$

The solid line on the right panel in Fig. 2 is the result of a least squares fit to the data. This approximation leads to $\gamma_0 = \gamma(P_{\mathrm{mean}} = 1\mathrm{GV}) = 11.2 \pm 0.5\%$/year and $\beta = -0.99 \pm 0.06$. These parameters are used to calculate the temporal variation in the rigidity range of each KET channel. As an example Fig. 3 shows the temporally detrended counting rates of >106 MeV protons (upper panel) in comparison with the counting rate ratios of KET to IMP8 UoC (lower panel). This figure shows that there is a good agreement between the measured counting rate ratios and the temporally detrended counting rates. The line in the figure reflect the spatial variation as discussed in detail in the following section.

3.2. Spatial variation along the Ulysses trajectory

The main goal of this paper is to investigate the spatial variation of galactic cosmic rays along the Ulysses trajectory as a function of particle rigidity during solar minimum conditions. Because KET and the UoC instrument on IMP8 do not measure particles in the same energy windows we used Eq. 2 to detrend the counting rates from the longterm recovery of galactic cosmic rays, as described in the previous section. As mentioned above, Fig. 3 shows in the upper panel the normalized, temporally detrended >106 MeV proton counting rates, which reflects the spatial variation of galactic cosmic ray protons along the Ulysses trajectory. The solid line in the upper panel of Fig. 3 shows an approximation of the detrended counting rates by the following function:

$$C(t) = C_{\infty}\left(1 - A/100 \cdot \exp\left((t - t_0)^2/\sigma^2\right)\right) \tag{3}$$

$C_{\infty}\left(1 - A/100\right)$ in Eq. 3 is the normalization factor we used in Fig. 3 evaluated for $t = t_0$, where t_0 corresponds to the time of minimum fluxes, and σ reflects the time scales of spatial variation along the Ulysses trajectory. In the special case of >106 MeV protons the fit leads to the following parameters:

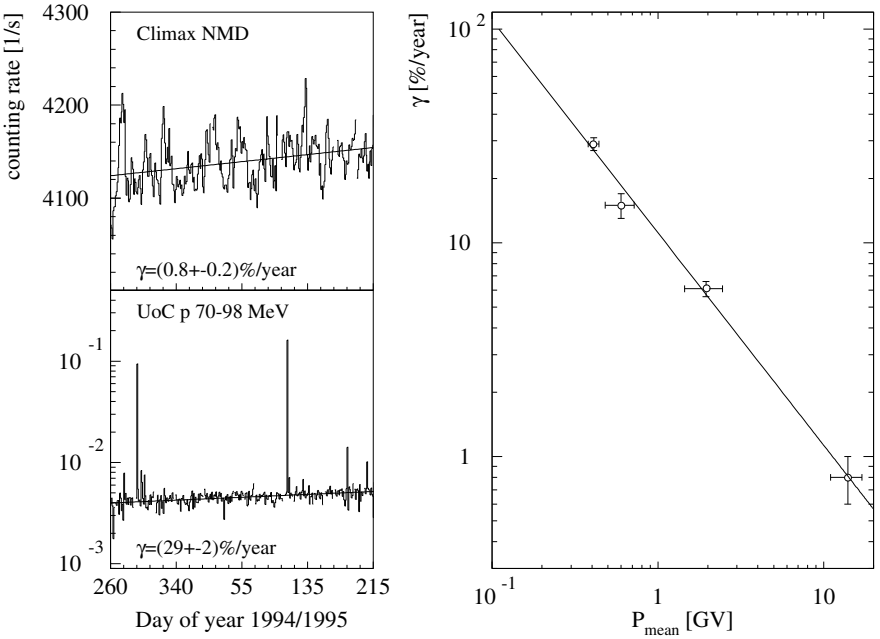

Fig. 2. Left: daily averaged counting rates measured by the UoC instrument on board IMP8 and UoC Climax neutron monitor and approximation by Eq. 1. Right: variation γ in %/year of daily averaged counting rates from the UoC instrument on IMP 8 and the UoC Climax neutron monitor.

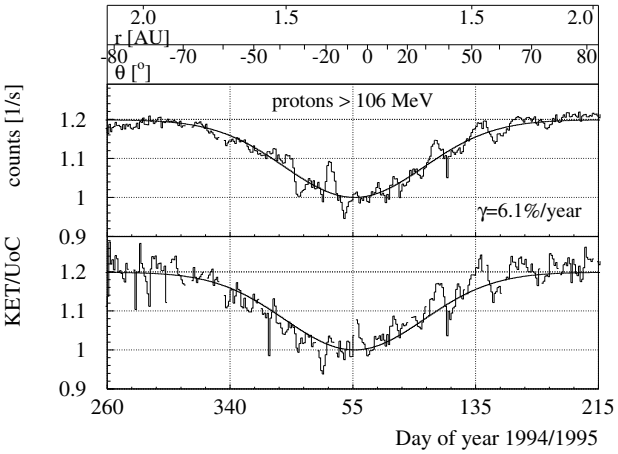

Fig. 3. Upper panel: temporally detrended daily averaged couting rate for >106 MeV protons and approximation by Eq. 3. Lower panel: daily averaged counting rate ratio of >106 MeV protons and same approximation as in the upper panel.

C_∞ = (0.27 ± 0.02) c/s, A = 16.6 ± 1, (t_0 = 1878 ± 0.5) days[1], and σ = (67 ± 1) days. It is important to note that t_0 corresponds to a Ulysses heliographic latitude of ∼10° S and not to 0°. In Heber et al. (1996) we have investigated the spatial variation of >106 MeV protons in detail and found that the spatial variation along the Ulysses trajectory is symmetric to a surface with an angle of 7°S. In the lower panel of Fig. 3 the daily averaged counting rate ratio of KET to IMP 8 UoC >106 MeV protons is shown. Superimposed is the result of the fit to the temporally detrended counting rates (copy from the upper panel). One can see how excellent the general trend of the observations — apart from the superimposed effect by CIRs — is fitted by the simple form of Eq. 3. It also reproduces the results found for >106 MeV protons by Heber et al. (1996) and Paizis et al. (1995):

1. The KET to UoC IMP 8 ratio is roughly constant over the latitude range extending from 30°S to 10°N.
2. The latitudinal gradient decreases for latitudes Θ >60°.

As we show below, latitudinal gradients G_θ can be calculated from the ratio of the counting rates over the poles C_{mpl} to the counting rates at low latitudes C_0. The physical ratio C_{mpl}/C_0 is a function of the mathematical fit parameter A. This follows from the fact that the difference in time between t_0 and t_{mpl} (maximum polar latitude) is ∼150 days or ∼2.3σ. Under this condition the ratio C_{mpl}/C_0 of the corresponding counting rates at 80° and close to the ecliptic plane is well approximated by

$$C_{mpl}/C_0 \approx C_\infty/C_0 = 1/(1 - A/100) \quad (4)$$

In our subsequent discussion we keep t_0 and σ as calculated above, independent of particle species and energy. The check of this assumption would require a detailed analysis of every KET channel as done for >106 MeV protons in Heber et al. (1996). Such an analysis is not possible for some of the KET channels, either because of a missing baseline near 1 AU or because of very low counting rates. Therefore, we do not claim that for the whole rigidity range covered by KET the spatial variation is symmetric to 7°S. But as will be demonstrated below, the usage of this assumption is consistent with the various data sets, and in this way we can describe the behaviour of the individual KET channels simply by variations in the parameters A and C_∞.

We show in Fig. 4 for helium nuclei in the energy range of 38–125 MeV/n and above 2000 MeV/n the fit according to Eq. 3. Even under the constraints discussed above the fit leads to a good approximation. However, we see the same general trend as in Fig. 3, but different ratios C_{mpl}/C_0.

Table 3 summarizes the results of the fit to all KET channels. Fig. 5 shows the approximate temporally detrended and

[1] t_0 gives the number of days since 1-Jan.1990

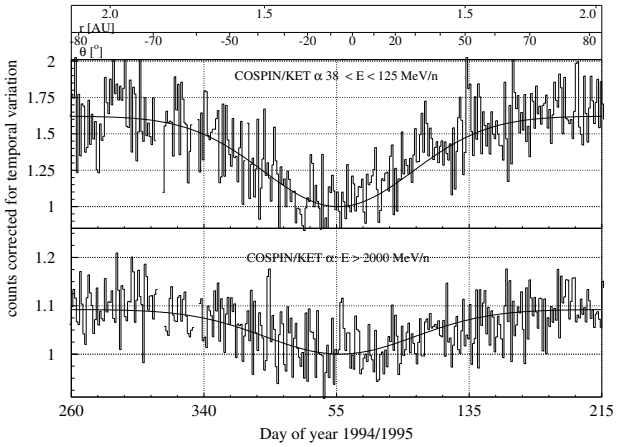

Fig. 4. Temporally detrended daily averaged counting rates for helium nuclei in the energy range 38–125 MeV/n (upper panel) and >2000 MeV/n and approximation by Eq. 3.

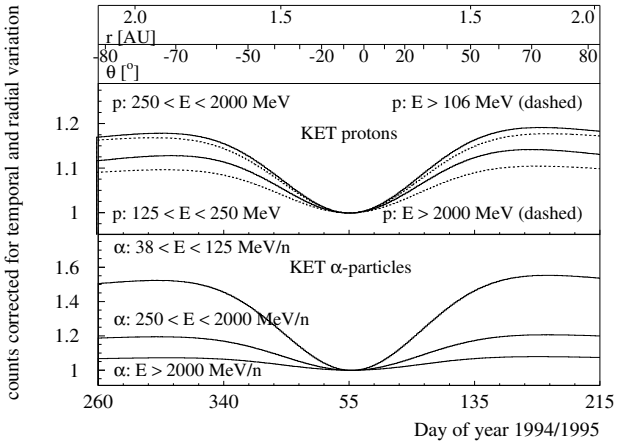

Fig. 5. Approximation (Eq. 3) for temporally detrended counting rates of protons (upper panel) and helium nuclei (lower panel) as a function of Ulysses heliographic latitude. The two lowest curves in the upper panel are for 125–250 MeV (solid line) and for >2000 MeV protons (dashed line). Protons in the energy range of 250–2000 MeV have the largest polar flux excess.

normalized counting rates of all KET channels (apart from 38–125 MeV protons) as a function of Ulysses heliographic latitude, with proton channels in the upper panel, helium nuclei in the lower panel. Fig. 1 had shown that the observed time profile of 38–125 MeV protons is markedly different from the profile of >106 MeV protons. The counting rate time profile is mostly dominated by temporal changes. Therefore the proton channel 38–125 MeV is not shown in Fig. 5. Note that the alpha channel 38–125 MeV/n is mainly dominated by the anomalous component. For α-particles the spatial excess decreases with increasing rigidity. However, protons show a different behaviour: the two lowest curves in the upper panel of Fig. 5 are for 125–250 MeV (solid line) and for >2000 MeV protons (dashed line). Protons in the energy range of 250–2000 MeV have the largest polar flux excess and also the highest absolute fluxes (see Fig. 5 in Simpson et al. 1995b).

In interpreting this result, one has to take into account that the spatial variation has two reasons:

1. Radial gradients: during the time period from September 1994 to July 1995 Ulysses moved from 2.3 AU to 1.3 AU at the ecliptic crossing and back to 2 AU. This point will be discussed in Sect. 3.3.
2. Latitudinal gradients: during this time period Ulysses scanned the inner heliosphere very quickly from 80°S to 80°N, leading to a true latitudinal variation as discussed in Sect. 3.4.

3.3. Radial gradients along the Ulysses trajectory

Since the beginning of 1994 solar activity has been low. In the beginning of 1994 Ulysses was above 50°S and at a radial distance of 3.8 AU. The detailed analysis in Heber et al. (1996) and Paizis et al. (1995) shows that the latitudinal variation above 60° heliographic latitude is small. From day 145 to day 197 of 1994 Ulysses moved from 65°S to 73°S at a radial distance of ∼2.9 AU. The spacecraft scanned the same latitude range again from day 296 to day 325 of 1994 at a radial distance of ∼1.9 AU.

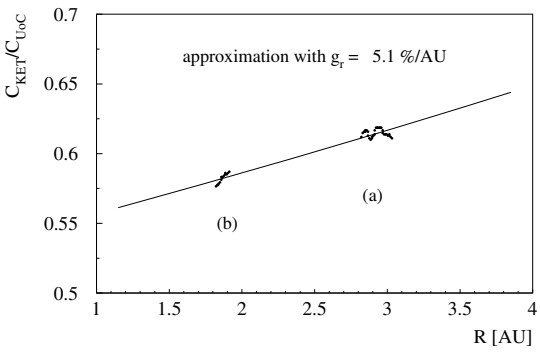

Fig. 6. Ulysses to IMP 8 ratio as a function of Ulysses radial distance. The solid line is the fit of Eq. 5 to the data with a radial gradient g_r = 5.1%/AU. (a) data taken between 65°S and 73°S during day 145–197 of 1994. (b) data taken from 73°S and 65°S during the fast latitude scan.

This gives the unique opportunity to calculate radial gradients at high solar latitudes. In Fig. 6 the 26-day running mean averaged counting rate ratio of >106 MeV protons as a function of radial distance is shown. Under the assumption made above this ratio can be approximated by:

$$C_{KET}/C_{UoC} = N \exp(g_r r) . \quad (5)$$

For >106 MeV protons the fit of Eq. 5 to the data leads to a radial gradient of 5.1%/AU. To estimate the uncertainty of g_r we varied the latitude window between 65°and 78° over which the average is taken. By this method we get values for g_r from 3.7–5.1%/AU with a median of 4.4%/AU. Within the error bars this value is consistent with the radial gradient $g_r = 3.2 \pm 0.8$ and 3–3.5%/AU obtained by Heber et al. (1993) and Paizis et al. (1995) for the *in-ecliptic* part of the mission in 1991 and 1992 and at higher latitudes in 1993 and 1994.

Table 3. C_∞/C_0 from Eq. 5, radial gradients g_r, and resulting latitudinal gradient $\overline{G_\Theta}$ for the analysed KET channels (see text for details).

part.	E_{min} MeV/n	E_{max} MeV/n	C_∞/C_0	g_r %/AU	$\overline{G_\Theta}$ %/°	G_Θ %/°
p	38	125	1.07	7.5[c,d]	0.03	0.11
p	125	250	1.17	5.5	0.15	0.30
p	250	2000	1.22	4.9[c]	0.21	0.38
p[a]	250	450	1.20	4.9[c]	0.20	0.35
p[a]	400	1000	1.24	4.9[c]	0.24	0.40
p[a]	800	2000	1.22	4.9[c]	0.18	0.37
p	> 106		1.20	4.4[c,d]	0.19	0.35
p	> 2000		1.12	3.3[c]	0.12	0.22
α[b]	38	125	1.65	3.0[c,d]	0.61	0.95
α	250	2000	1.23	4.7[c]	0.23	0.40
α	> 2000		1.09	2.5[c,d]	0.09	0.16

[a] PHA selected part of 250–2000 MeV protons, gradients are assumed to be the same as for 250–2000 MeV protons.
[b] dominated by the anomalous component.
[c] measurements in 1991–1994
[d] measurements from solar cycle 20, see text for details

We use the same procedure to calculate the radial gradients at high latitudes for 70–98 MeV protons and 38–98 MeV/n helium nuclei. We find g_r = 7.5 ± 1.5%/AU for the proton channel and g_r = 3.0 ± 1.4%/AU for the α-channel. During the in-ecliptic part of the Ulysses mission the Sun was more active, so that there were insufficient periods of time to obtain statistically significant radial gradients for these channels. The High Energy Telescope on board Ulysses has a 5–10 times larger geometric factor than the KET. They found for 31–70 MeV/n helium nuclei a radial gradient of 4.6%/AU (see McKibben et al. 1995).

It is interesting to compare our results with results from the Pioneer spaceprobes, which were launched 22 years ago. At that time the Sun also approached solar minimum conditions and the solar magnetic field had the same configuration ($A > 0$). The values for the in-ecliptic radial gradients 22 years ago (see Fig. 3 in McKibben 1986) are 4–10%/AU for 30–70 MeV protons, 3–5%/AU for >70 MeV protons. This means that radial gradients at high latitudes are not significantly different from radial gradients determined in the ecliptic plane, confirming our assumption introduced above that radial and latitudinal variations are separable.

In Table 3 we summarize the radial gradients used in the following analysis. These values are taken from the in-ecliptic and higher latitude part of the mission (Heber et al. 1993 and Paizis et al. 1995), and from Pioneer and neutron monitor measurements 22 years ago during a comparable phase of the solar cycle (McKibben 1986, McDonald et al. 1992, Fujii & McDonald 1995 and Hall et al. 1995).

3.4. Latitudinal gradients

As discussed above, we fixed σ and t_0 in the fitting procedure, so that the temporally corrected counting rate at 80°N and S is given by C_∞/C_0 for all KET channels. Taking into account the restrictions summarized above we can calculate an averaged latitudinal gradient by the following equations:

$$C(r,\Theta) = C_0 \exp\left(g_r \cdot (r - r_0) + G_\Theta(\Theta - \Theta_0)\right) \quad (6)$$

From this we obtain:

$$G_\Theta = \left(\ln\left(C(r,\Theta)/C_0\right) - g_r \cdot (r - r_0)\right)/(\Theta - \Theta_0)$$

and for
Θ = 80° we get

$$\overline{G_\Theta} = \left(\ln\left(C_\infty/C_0\right) - g_r \cdot (r - r_0)\right)/(\Theta - \Theta_0) \quad . \quad (7)$$

Here the values of r range from r_0 to r_{mpl} where r_0 = 1.34 AU is the closest approach of Ulysses to the Sun during the fast latitude scan, r_{mpl} = 2.28 AU and 2.01 AU, are the Ulysses radial distances for the 80°South and North polar passages, respectively. $\Theta_0 \approx 7°$ is taken to be independent of particle type and energy (see the discussion above). In Heber et al. (1996) we showed for >106 MeV protons that the latitudinal gradient is a function of latitude. As stated above we do not claim that the function given in Eq. 3 reproduce the exact latitudinal profile of each KET channel. However to estimate the variation of the latitudinal gradient G_θ with latitude, we calculate G_θ around the turning points of function 3. This can be interpreted as the maximum value for the latitudinal variation. The latitudinal gradients in Table 3 are the mean values for the northern and southern hemisphere taking into account the different radial distances at southern and northern polar regions. The rigidity dependence of protons in the energy range of 250–2000 MeV is of particular interest. Therefore, we subdivide this energy range into three sub-channels using pulse height analysis information.

The rigidity dependence of the averaged latitudinal gradient $\overline{G_\Theta}$ and the maximum latitudinal Gradient G_Θ is shown in Fig. 7 left and right, respectively. Errors in the determination of $\overline{G_\Theta}$ and G_Θ result from uncertainties in A and in g_r. The error bars in Fig. 7 are based on the following estimates: (1) The temporal rate of increase γ is known with a certain accuracy. Fitting Eq. 3 to the temporally corrected counting rates according to the corresponding limits in γ leads to a smaller parameter A, because the function described by Eq. 3 is symmetric in time with respect to t_0. The uncertainty in A is for all KET-channels of the order of 5%. (2) We assume that the radial variation is small compared to the latitudinal variation. This is true for all channels except 38–125 MeV protons. A radial gradient of ∼10%/AU could explain the measured C_∞/C_0. To estimate the uncertainty of $\overline{G_\Theta}$ because of the variation in G_r we calculate $\overline{G_\Theta}$ using the values given in Table 3 and a constant value of 2.5%/AU. This leads to a total uncertainty of $\overline{G_\Theta}$ of ∼10% for all channels analysed, except the 38–125 MeV protons. For this energy channel we get an upper value of $\overline{G_\Theta}$ of 0.05%/° for g_r = 2.5%/AU and a value of 0.01%/° for g_r = 7.5%/AU resulting in an uncertainty of about 100%.

Simpson et al. (1995a) determined the latitudinal gradient using data from the COSPIN High Energy Telescope from the

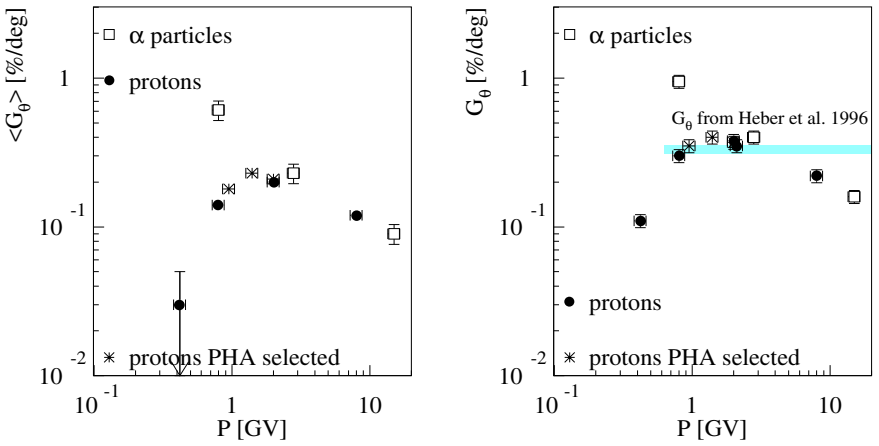

Fig. 7. Rigidity dependence of the average latitude gradient $< G_\theta >= \overline{G_\Theta}$ (left) and the maximum latitudinal gradient G_Θ (right). The symbols •, □ and ⋆ mark the results from the proton, alpha-particle channels, and from the pulse height analysis of 250–2000 MeV protons. Marked in the right panel is the value G_θ found by our analysis in Heber et al. (1996).

southern part of the fast Ulysses latitude scan. They found for 35–70 MeV/n protons and helium nuclei a latitudinal gradient of $-0.08 \pm 0.09\%/^\circ$ and $0.57 \pm 0.1\%/^\circ$ and for 70–90 MeV/n protons and helium nuclei a latitudinal gradient of $0.05 \pm 0.06\%/^\circ$ and $0.38 \pm 0.07\%/^\circ$, respectively. These values are within the errors consistent with the values we found for corresponding channels (see Table 3). G_θ for >106 MeV protons calculated at the turning points of function 3 is consistent with the value found by our previous analysis in Heber et al. (1996). For helium nuclei $\overline{G_\Theta}$ decreases with increasing energy, whereas for protons the behaviour is different. Here we see a clear maximum in the latitudinal gradient for protons around 1.5 GV.

4. Comparison of observations with modulation models

In this section the results deduced from the KET measurements are compared to results of modulation models. The advantage of the fast Ulysses latitude scan is that during this time of the solar cycle for most particle species and energies variations in time are small compared to those in space. This gives us a unique data set to study spatial modulation processes. For a first comparison of the observations with model predictions we calculate the flux variation along the Ulysses trajectory using a steady-state modulation model.

4.1. Model description

We start with a steady-state drift modulation model as described in Burger & Potgieter (1989). In this model, the Parker transport equation (Parker 1965) was solved with a numerical code which included *i)* convection in a solar wind varying with latitude, *ii)* diffusion due to the irregularities of the HMF, *iii)* gradient and curvature drifts in the background HMF and *iv)* adiabatic energy losses due to the expanding solar wind. As discussed in Haasbroek et al. (1995) a parameter set where both $\kappa_\parallel$ and $\kappa_\perp$ vary $\propto 1/B$, with B the magnitude of the HMF, led to a latitudinal variation of cosmic-ray intensities along the Ulysses trajectory which was too large. The basic set of parameters was also used for the present computations. The rigidity dependence of the diffusion coefficients was conveniently chosen as $\propto P$ above 0.4 GV and constant below this value. Our model heliosphere was bounded at 100 AU where an interstellar source spectrum was assumed. For this study we used *i)* an Archimedean spiral HMF (Parker geometry), until recently assumed to represent the global structure of the HMF and *ii)* a modified HMF according to the spiral angle modification proposed by Smith & Bieber (1991). This modification leads to qualitatively similar results as the one proposed earlier by Jokipii & Kota (1989) (see Haasbroek & Potgieter 1995).

4.2. Model results and discussion

For our analysis we used the normalised counting rates from Sect. 3 for protons in different energy windows. Fig. 8 shows in the left panels the model results (solid lines) and the data as approximated by Eq. 3 (dashed lines). The model results with the Parker HMF are indicated by (a), with the Smith and Bieber modification by (b). It is obvious that in all cases the variation of the galactic cosmic ray flux is lower than the variation predicted by the Parker HMF model. Results from the magnetic field experiment on Ulysses show that the description of the large scale magnetic field by the Parker spiral geometry is too simplified. In addition, large fluctuations of the magnetic field are observed at high latitudes (see e.g. Balogh et al. 1995, and Horbury et al. 1995). Jokipii & Kota (1989) had already suggested the existence of large scale, transverse magnetic field fluctuations in the heliographic polar regions. This would impede the access of cosmic rays from the polar regions, particularly during an $A > 0$ magnetic solar cycle.

With the Smith & Bieber (1991) modified HMF the model describes the observation for >2000 MeV protons very well. For lower energy protons the predicted fluxes at polar latitudes are too high for both magnetic field models.

Fig. 8 on the right shows the rigidity dependence of the polar flux enhancement C_∞/C_0 with respect to the equatorial plane (for definition see Eq. 3, values are summarized in Table 3). We restrict our comparison to proton measurements because of simplicity. Symbols denote measurements, lines denote model results. In the model calculations all energies were integrated for the >2000 MeV and >106 MeV proton channels. As stated

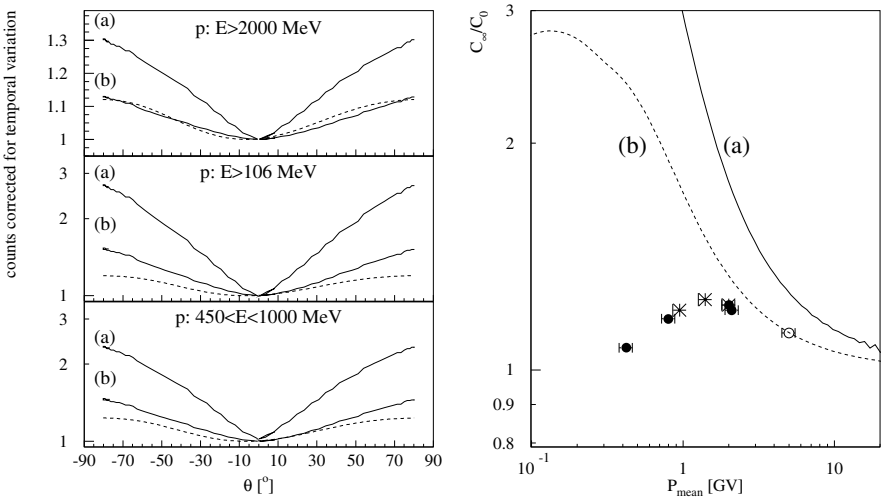

Fig. 8. Left: Variation of cosmic ray flux along the Ulysses trajectory in different KET proton channels as a function of Ulysses latitude. Right: Rigidity dependence of C_∞/C_0. The solid and dashed lines give the result of a steady-state drift modulation model with (a) a Parker HMF and (b) a modified HMF according to Smith and Bieber. The symbols • and ⋆ mark the results from the proton channels,and from the pulse height analysis of 250–2000 MeV protons. The >2000 MeV proton channel (□) is put on top of curve (b). For details see text.

above we found a good agreement for >2000 MeV protons. Therefore we put this channel (indicated by an open box) on top of the dashed curve.

It is obvious that measurements are not reproduced by the model calculations at low rigidities, and the discrepancies increase with decreasing rigidity. Apart from allowing too little modulation over the poles in our model, this indicates that the assumed rigidity dependence for the diffusion coefficients was too simple. Computations in Ferrando et al. (1996) showed that a rigidity dependence $\propto P^{0.3}$ gave better compatibility with observations for the range 0.9–2.5 GV. Alternatively, time-dependent modulation effects might still have a strong effect at these low energies, see the results in Fig. 1 where the protons below 125 MeV are still recovering fast. Examples of time-dependent effects are: the extent to which drift effects are operating as a function of time, the amount of perpendicular diffusion, especially in the polar direction, with respect to parallel diffusion, the temporal evolution of turbulence in the polar regions with respect to the equatorial plane and the recovery of low rigidity particles with respect to high rigidity particles (Le Roux & Potgieter 1992 and Potgieter & Le Roux 1992). We will discuss these features in more detail in subsequent papers. In particular, the relative importance of different effects causing the modulation will be analysed.

5. Summary

We have analysed KET measurements of >40 MeV/n nuclei over the time period from mid 1994 to mid 1995 and compared them with results from a steady state modulation model calculation. In spite of the relatively short time period of the Ulysses' fast latitude scan temporal variations have been taken into account. The analysis leads to the following results:

- The flux enhancement of ∼10–60% observed at high latitudes are caused by latitudinal variation.
- For α-particles the latitudinal gradient is increasing from 0.16%/° for >2 GeV/n to 0.95%/° for 38–125 MeV/n α-particles.
- For protons the magnitude of the latitudinal gradient varies between 0.11%/° and 0.4%/° with a maximum for 1.5 GV protons.
- We used a two-dimensional steady-state modulation model which describes the variation of >2 GeV very well, but cannot reproduce the measured rigidity dependence of the latitudinal enhancement of proton intensities. This indicates that the assumed rigidity dependence for the diffusion coefficients in our model was too simple and/or that time-dependent modulation effects should also be taken into account.

Acknowledgements. We are grateful to B. McKibben, J. Simpson, C. Lopate, R. Pyle, and T. Hoeksema for making available IMP-8 particle and Climax neutron monitor data and magnetic tilt angles. University of Chicago IMP-8 and Climax neutron monitor data were prepared in part using funds from NASA Grant #NAG 5-706 and NSF ATM 94-20790. This work was partly supported by Deutsche Agentur für Raumfahrtangelegenheiten (DARA) under grant No. 50 ON 9106.

References

Balogh A., Smith E.J., Tsurutani B.T., et al., 1995, Science 268, 1007
Burger R.A., Potgieter M.S., 1989, ApJ 339, 501
Burger R.A., Hattingh M., 1995, Astrophys. Space Sci. 230, 375
Dröge W., Kunow H., Heber B., et al., 1995, Solar Wind 8, in press
Ferrando P., Raviart A., Haasbroek L.J., et al., 1996, A&A, this issue
Fujii Z., McDonald F.B., 1995, Proc. of the 24th Int. Cosmic Ray Conf. (Rome) 4, 772
Haasbroek L.J., Potgieter M.S., 1995, Space Sci. Rev. 72, 385
Haasbroek L.J., Potgieter M.S., Wibberenz G., 1995, Proc. of the 24th Int. Cosmic Ray Conf. (Rome) 4, 768
Hall B., Duldig M.L., Humble J.E., et al., 1995, Proc. of the 24th Int. Cosmic Ray Conf. (Rome) 4, 611
Heber B., Raviart A., Paizis C., et al., 1993, Proc. of the 23rd Int. Cosmic Ray Conf. (Calgary) 3, 461
Heber B., Dröge W., Kunow H., et al., 1996, Geophys. Res. Lett., in press
Horbury, T.S., Balogh, A., Forsyth, R.J., et al., 1995, Geophys. Res. Lett. 22, 3401
Jokipii J.R, Kóta J., 1989, Geophys. Res. Lett. 16, 1

Le Roux J.A., Potgieter M.S., 1992, ApJ 390, 661
McDonald F.B., Moraal H., Reinecke J.P.L., et al., 1992, J. Geophys. Res. 97, 1557
McKibben R.B., 1986, in: "The sun and heliosphere in three dimensions", R.G. Marsden Ed., Reidel Publ. Cy., p.361
McKibben R.B., 1989, in: "Physics of the outer heliosphere", S. Grzedzielski and D.E. Page Eds, Pergamon Press, p.107
McKibben R.B., Simpson J.A., Zhang M., et al., 1995, Space Sci. Rev. 72, 403
Parker E.N., 1965, Plan. Space Sci. 13, 9
Paizis C., Heber B., Raviart A., et al., 1995, Proc. of the 24th Int. Cosmic Ray Conf. (Rome) 4, 756
Potgieter M.S., Le Roux J.A., 1992, ApJ 392, 300
Potgieter M.S., 1995, Astrophys. Space Sci. 230, 393
Rastoin C., Ferrando P., Raviart A., et al., 1996, A&A 307, 981
Sanderson T.R., 1995, Adv. Space Res. 16, 267
Simpson J.A., Anglin J.D., Balogh A., et al., 1992, A&AS 92, 365
Simpson J.A., Connell J.J., Lopate C., et al., 1995a, Geophys. Res. Lett. 22, 3337
Simpson J.A., Anglin J.D., Bothmer V., et al., 1995b, Science 268, 1019
Smith C.W., Bieber J.W., 1991, ApJ 370, 435
Zhang M., Simpson J.A., McKibben R.B., et al., 1995, Proc. of the 24th Int. Cosmic Ray Conf. (Rome) 4, 956